Available online at www.sciencedirect.com

ScienceDirect

Procedia Engineering 144 (2016) 1138 – 1149

Procedia Engineering

www.elsevier.com/locate/procedia

12th International Conference on Vibration Problems, ICOVP 2015

Design of Suspension System for Formula Student Race Car

Samant Saurabh Y., Santosh Kumar, Kaushal Kamal Jain, Sudhanshu Kumar Behera, Dhiraj Gandhi, Sivapuram Raghavendra, Karuna Kalita*

IIT Guwahati, Guwahati, Assam-781039, India.

Abstract

In this work, we presented in detail the design procedure of the front double A-arm push rod suspension system for a formula student race car. The type of suspension systems used generally are reviewed. The CAD models of the components in the suspension system are made using SolidWorks® and the Finite element analysis of the components is done using ANSYS® Workbench. Both kinematic and dynamic analysis of the designed suspension system is performed. The results of vibration or ride analysis and roll steer analysis are also presented for the designed suspension system. The method for spring design is elucidated. This work emphasizes the method for designing and analyzing the suspension system for a race car in various aspects.

Peer-review under responsibility of the organizing committee of ICOVP 2015

Keywords: Pushrod; Pullrod; A-Arm; Caster; Camber; Toe.

1. Introduction

A Formula student race car is a simplified version of Formula One race car designed and built by the university students for competitions like FSAE, Supra SAE, and Formula Student etc. Suspension plays a major role during race car racing. Generally, in race a car, double wishbone suspension with either pullrod or pushrod is used owing to ease of design and lighter components involved [1]. However, various combinations of pushrod and pullrod

* Corresponding author.
*E-mail address:*karuna.kalita@iitg.ernet.in

Peer-review under responsibility of the organizing committee of ICOVP 2015
doi:10.1016/j.proeng.2016.05.081

suspensions have been used in the front and the rear. For example, as mentioned in [2], Formula one cars generally use pushrod is used in the front because with pull rod in rear. As evident from [3, 4, 5] this combination is quite popular in formula student vehicles too. Some student formula vehicles like [6, 7, 8], have used a reverse combination i.e., pullrod in front and pushrod in rear. Many formula student cars as in [9, 10, 11] also use either pushrod or pullrod suspension in both front and rear. This paper presents the procedure of design and analysis (both kinematic and dynamic) of the front double A-arm push-rod suspension system for a formula student race car.

The design of suspension of a race car is complex; hence there is a need to have a procedure by following which the suspension system can be designed. This paper proposes a procedure which involves kinematic and dynamic analysis followed by vibration analysis for the design of a Double A-arm pushrod suspension system. The results include kinematic position of linkages and specifications of spring-damper. These results were validated through roll steer analysis of the suspension. In most of the literature like [12], the kinematic analysis of double wishbone suspension is carried out by assuming the suspension geometry to be a two dimensional 4 bar mechanism. However, this analysis is an approximation because of the presence of spherical joints in the actual suspension system. Hence, in the proposed procedure, the kinematic analysis was done using three dimensional graphical method and the change in wheel alignment was plotted with the wheel travel [13]. From the static and dynamic analyses, stiffness of the spring was calculated. Damping ratio was calculated by analyzing the quarter car model of the vehicle. The calculated values of stiffness and damping ratio were validated through roll steer analysis.

2. Design

2.1. Design Expectations

The suspension is designed so as to satisfy following design criterion:

- Easy to design and manufacture
- Usable wheel travel of at least 50.8 mm, 25.4 mm jounce and 25.4 mm) rebound.
- Roll centre sufficiently above ground for good lateral stability.
- Small variations in camber and toe angles during the desired wheel travel.

2.2. Design Expectations

- Co-ordinates of mounting points and dimensions of A-arms and pushrod.
- Height of roll centre from the ground and wheel alignment (caster, camber and toe angle) at car’s standstill position with a 75 kg person seated inside.
- Dimensions of the knuckle.
- Co-ordinates of mounting point and dimensions of the bell crank.
- Spring constant and damping ratio of the spring-damper.

2.3. Design Procedure

Height of the roll centre was decided to be 50mm from the ground. Generally race car prefers negative camber in order to have lateral force and toe out due to ease while turning. The values of camber, caster and toe angles were decided to be -1o, 5o and 1o [13]. These values would be attained when the vehicle is in a standstill position with a 75 kg person seated inside. Taking these design decisions as constraint, an iterative design procedure was followed to make the rest of the design decisions. The first decision to be made was the coordinates of mounting points and dimensions of the A-arms. From the survey of commercially available knuckles, the King Pin inclination of 7o and vertical distance between mounting points of lower and upper A-arms of 205mm along with a track width of 1200mm was chosen for the first iteration. The coordinate system shown in Fig.1 was followed throughout the procedure.

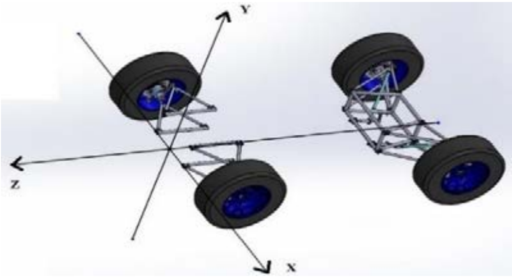

Figure 1. Coordinate System and CAD Model of the Final Suspension Design

The mounting points of the A-arms on chassis were labelled as shown in Fig. 2. Keeping the length CD fixed, lengths AB, BC and AD were varied and graphs were plotted for variations in the wheel alignment with the wheel travel, using the kinematic analysis carried out in section 2. The geometry with minimum variation in wheel alignment with wheel travel was finalized.

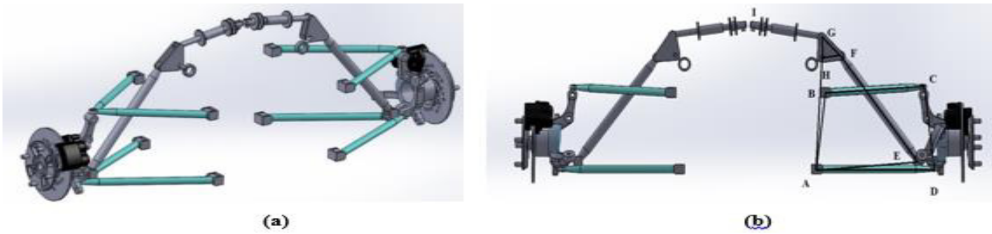

Figure 2. Front Suspension (a) Isometric view (b) Front view with labelling

The next decision to be made was the coordinates of mounting points and dimensions of pushrod and bell crank. One end of the pushrod was mounted on the lower A-arm at point E. Due to the space constraints on the chassis, the maximum length of spring (IG) was fixed and the maximum compression of the spring was decided to be 25.4mm.

Thus the final problem was the maximum and minimum angles of line HG for 25.4mm movement of the spring. The maximum and minimum angles of line AE was also known for 25.4mm jounce and 25.4mm rebound. Thus, it was a problem of four bar mechanism in which the length of central link (HA) was fixed and the range of angles for input link (GH) and output link (AE) known. The problem was solved by geometrical constructions to find the point F as the mounting point of push rod on bell crank. Thus the shape of bell crank was decided. After deciding the geometry, the finite element analysis of each link and the performance of suspension (ride, roll and pitch analysis) were carried out using dynamic analysis demonstrated in section 4. An iterative procedure was carried out until satisfactory kinematic and dynamic results were obtained.

3. Kinematic Analysis

3.1. Aim

The kinematic analysis of the suspension was carried out to:

- Evaluate the change in wheel alignment i.e. Caster, Camber and Toe angles during the wheel travel of 75mm (37.5mm jounce and 37.5mm rebound) and steering.

- Check the maximum and minimum length of the spring during wheel travel.

The minimum and maximum length of the spring were directly measured from SOLIDWORKS® software by keeping the wheel at lowest (max jounce) and highest point (max rebound). Hence the kinematic analysis was carried out to check the wheel alignment.

3.2. Evaluation of change in wheel alignment

The kinematic structure of the pushrod suspension (relevant for wheel alignment analysis) is represented by Fig. 3.

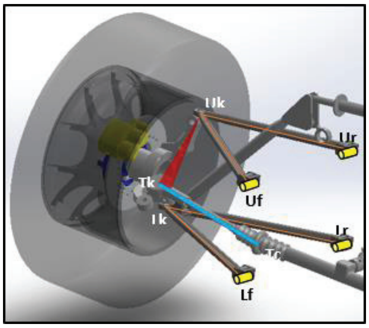

Figure 3. Kinematic Structure of Pushrod Suspension

Since, the suspension consists of Z-axis pin joints (Ur, Uf, Lr and Lf) as well as spherical joints (Uk, Lk, Tk and Tc), it is a 3-D mechanism and hence, the kinematic analysis was carried out using 3-D graphical method. It was assumed that the coordinates of points Uf, Ur, Lr, Lf and Tc and the initial coordinates of Uk, Lk and Tk are known. In order to simplify the analysis, each A-Arm was represented as a single link (Uk-Uc or Lk-Lc) as shown in Fig.4. The modified kinematic structure is as shown in Fig.5.

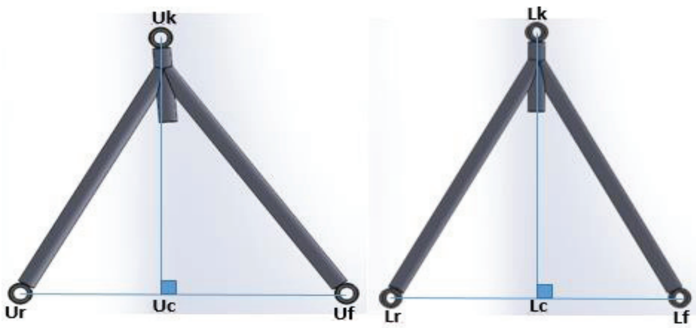

Figure 4. Simplified representation of A-Arms

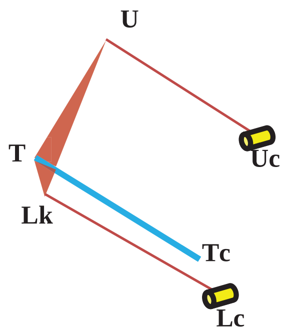

Figure 5. Modified Kinematic Structure of Suspension

Then, the following were to be calculated from the initial coordinates of all the points as they were used as constants during the analysis:

- Length of modified upper A-Arm (dU), lower A-Arm (dL) and Tie Rod (dT).
- Distance between Lk and Uk (dK).
- Perpendicular distance between Tk and the line joining Uk and Lk (dP).
- The ratio (r) in which perpendicular from Tk divides the line joining Uk and Lk.

With the points Lc, Uc and Tc fixed, and the aim of the kinematic analysis was to find the coordinates of points Lk, Uk and Tk so as to find the wheel alignment. For a given angle of lower A-Arm with the horizontal (θ) and taking Lc as origin, the coordinates of Lk came out to be ($-dL\cos\theta$, $-dL\sin\theta$, 0). Out of the two points of intersection of the sphere with centre as Lk and radius dK and the circle with centre as Uc, radius dU and axis as Z-axis; the point that was closer to the previous coordinates of Uk was chosen to be Uk. The point dividing the line joining Uk and Lk in the ratio r was named R. Out of the two points of intersection of the sphere with centre as Tc and radius as dT and the circle with centre as R, radius dP and axis as line joining Uk and Lk, the point that was closer to the previous coordinates of Tk was chosen to be Tk.

Caster was obtained by finding the angle between the projection of the vector Uk-Lk on YZ plane and Y axis. Camber was obtained by finding the angle between the projection of the vector Nk on XY plane and the X axis. Here Nk is the cross product of (Lk-Uk) and (Tk-Uk) and hence, the normal to the knuckle plane. Toe was obtained by finding the angle that the projection of the vector Nk on XZ plane made with the X axis. Using the above methodology, the wheel alignment was calculated for θ ranging from -5o to 5o and the plots of caster, camber and toe verse the wheel travel were obtained (Fig 11).

4. Static and dynamic analysis

The static and dynamic analysis was carried out in order to obtain the spring stiffness and calculate the maximum loads on each component respectively. Fx, Fy, Fz were taken as the lateral, vertical and longitudinal force acting on the wheel respectively. At the static condition, the vertical force acting on the wheel would be the total weight transfer on front wheel and the lateral and longitudinal forces acting on the wheel would be zero. From the force and moment balance equations about joints, forces on corresponding linkages were calculated [7]. All the terms used in the equations are explained in Appendix A (Ref Fig 6).

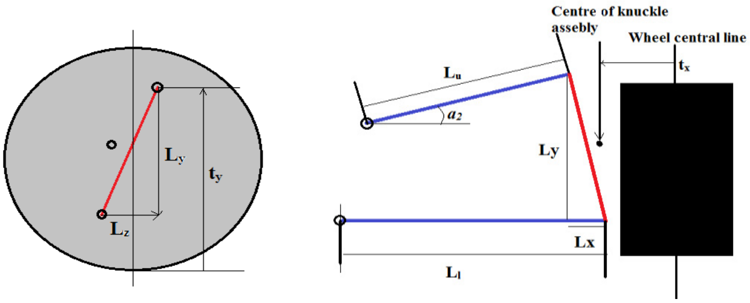

Figure 6. Wheel, A-arms alignment

$$\begin{bmatrix} 0 & 1 & 0 & 0 & 1 & 0 \\ 0 & 0 & 1 & 0 & 0 & 1 \\ 0 & 0 & 0 & 0 & Lz & Ly \\ 1 & 0 & 0 & 1 & 0 & 0 \\ 0 & 0 & 0 & Ly & Lx & 0 \\ tan\alpha_2 & -1 & 0 & 0 & 0 & 0 \end{bmatrix} \begin{bmatrix} F_{ux} \\ F_{uy} \\ F_{uz} \\ F_{lx} \\ F_{ly} \\ F_{lz} \end{bmatrix} = \begin{bmatrix} F_y - W_t \\ -F_z \\ -t_x(F_y - W_t) - F_z t_y \\ -(F_x + F_{st}) \\ -F_{st}s - t_x(F_y - W_t) - t_y F_x \\ 0.5W_{ua} \end{bmatrix} \tag{1}$$

By solving equation (1), all the forces acting on knuckle ball joints were obtained.

$$\begin{bmatrix} 0 & 0 & 0 & \frac{Lp}{Ll}(tan\alpha_1) & \frac{Lp}{Ll} & 0 \\ 1 & 0 & 0 & 1 & 0 & 1 \\ 0 & 1 & 0 & 0 & 1 & 0 \\ 0 & 0 & 0 & 1 & tan\Theta_f & 0 \\ 0 & 0 & 1 & 0 & 0 & 1 \\ 0 & 0 & 0 & 0 & tan\Theta_s & 1 \end{bmatrix} \begin{bmatrix} F_{pbx} \\ F_{pby} \\ F_{pbz} \\ F_{plx} \\ F_{ply} \\ F_{plz} \end{bmatrix} = \begin{bmatrix} F_{ly} + 0.5W_{ua} + F_{lx}tan\alpha_1 \\ 0 \\ Wp \\ -0.5Wp\, tan\Theta_f \\ 0 \\ -0.5Wp\, tan\Theta_s \end{bmatrix} \tag{2}$$

By solving equation (2), all the forces acting on push rod at lower A-arm end as well as at bell crank end were obtained. It was found that the force -F_{pb} acting on the bell crank by pushrod isn't coplanar with the bell crank. So to balance the torque about the hinged point of bell crank, the component of -F_{pb}, lying in the plane of the bell crank was calculated.

$$F = F_{bp} - n \times F_{bp} \tag{3}$$

Where, n is normal vector of the plane of the bell crank.

$$K_s = \frac{\left| r_{pb} \times F \right|}{\left\| r_{sb} \times \Delta x \right\|} \tag{4}$$

The final stiffness of the spring came out to be 40kN/m with spring compression 10mm. Similarly for rear suspension stiffness came out to be 60kN/m. In order to check the sustainability of the suspension linkages, the forces mentioned in [14] i.e. Fy = 3Mug, Fx = Fz = Mug were considered. Then the forces and moments on linkages were calculated using the procedure followed in the static analysis. These forces were considered while doing the FE analysis of the components in ANSYS®. A minimum factor of safety of 1.5 was taken to ensure the rigidity and strength of the suspension system while maintaining less weight.

5. Ride (Vibration) analysis

The ride analysis was carried out in order to calculate damping coefficient of the damper. Quarter car model of the suspension system was considered for this analysis (Fig 7). The damping coefficient of wheel was neglected as it is very small compared to the damping coefficient of the spring damper. The final equations of quarter car model are given below.

$$\frac{Z_s(s)}{Z_r(s)} = \frac{K_t(Cs+K)}{\left[(M_s s^2 + Cs + K)(M_u s^2 + Cs + K + K_t) - (Cs+K)^2\right]} \text{ [15, 16, 17, 18]} \tag{5}$$

$$\frac{Z_u(s)}{Z_r(s)} = \frac{K_t(M_s s^2 + Cs + K)}{\left[(M_s s^2 + Cs + K)(M_u s^2 + Cs + K + K_t) - (Cs+K)^2\right]} \text{ [15, 16, 17, 18]} \tag{6}$$

$$\frac{Z_s(s) - Z_u(s)}{Z_r(s)} = \frac{-K_t M_s s^2}{\left[(M_s s^2 + Cs + K)(M_u s^2 + Cs + K + K_t) - (Cs+K)^2\right]} \text{ [15, 16, 17, 18]} \tag{7}$$

$$\frac{Z_u(s) - Z_r(s)}{Z_r(s)} = \frac{-\left[(M_s s^2 + Cs + K)(M_u s^2 + Cs + K) - (Cs+K)^2\right]}{\left[(M_s s^2 + Cs + K)(M_u s^2 + Cs + K + K_t) - (Cs+K)^2\right]} \text{ [15, 16, 17, 18]} \tag{8}$$

Equation (5), (6), (7) and (8) indicates the sprung mass transmissibility, un-sprung mass transmissibility, sprung mass deflection, and tyre deflection respectively. To optimize the suspension system, plots of time response of equations (5), (7), (8) and frequency response of equations (5), (6) are plotted as shown in Fig 9 and Fig 10. From the time response, the range of damping ratio is selected in order to have damped state with the required time. In case of race cars, the damping should be fast enough to damp the oscillations in 0.2 to 0.5 seconds, hence a range of damping ratio [0.4 0.8] is selected (Fig 9). The frequency response of equations (3) and (4) are plotted across this selected range of damping ratio. Since, the rider comfort decreases with the increase in acceleration of the body, the amplitude of acceleration of the sprung mass was to be minimize. The peak amplitude of the wheel displacement at both the fundamental frequencies of un-sprung mass to be minimize in order to make sure that the wheel does not lose contact with the ground. As damping ratio of the damper increases, acceleration of sprung mass decreases; but at the same time un-sprung mass transmissibility also increases which may lose tyre contact with ground. Hence we need to select optimum damping ratio. Literature [17] states that, the damping ratio is optimum when the plot (Fig 10) across to resonance frequencies becomes almost linear so as to have less jerk at resonating frequencies. As shown in Fig 10, for damping ratio 0.7 the graph between the two natural frequencies becomes almost straight line. Hence the damping ratio becomes q = 0.7. Coefficient of damping is obtained which is, C = 0.7Co, where Co is the critical damping coefficient. Literature [20] states that a damping ratio of q= 0.7 has been used in the calculations based on discussions with industry professionals. This verifies our result.

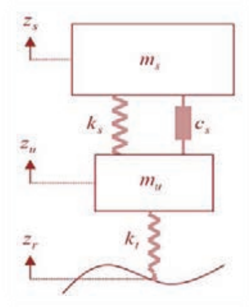

Figure 7. Quarter-car model

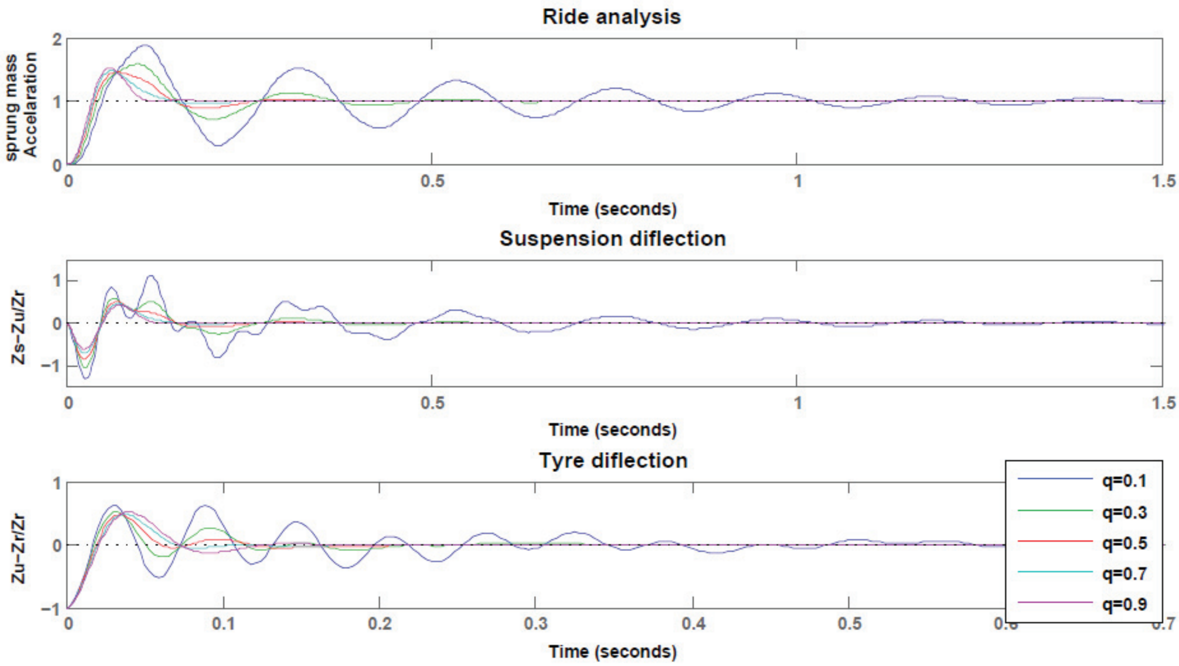

Figure 8. Time response of equations (5, 7, 8)

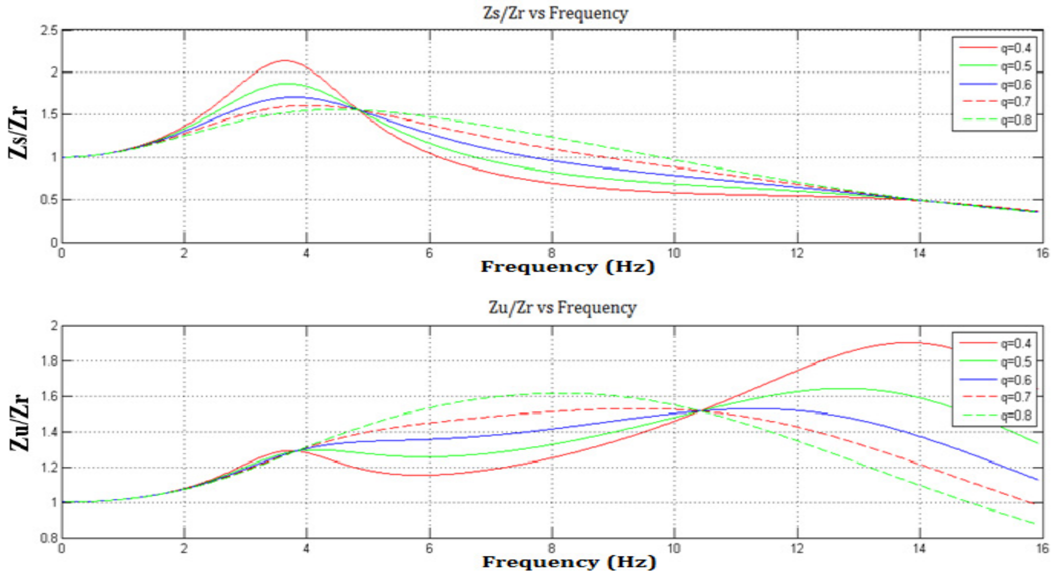

Figure 9. Frequency response of equations (5, 6)

6. Roll steer analysis

The roll steer analysis was carried out in order to validate the suspension designed through above procedure. When a car takes a turn, due to centripetal force acting on the centre of mass of the car there are unequal normal reactions acting on both the wheels. Due to this entire body rolls about roll centre of the car. This affects the driver comfort. In this analysis, we had considered velocity of car to be 80km/hr and radius of the turn 7m. Our expected criteria is that the roll angle should be below 10o.

Suppose, a car takes turn to left and body rolls at an angle Θ at the roll centre. Moment is balanced about roll centre and equation (5) generates:

$$I_{rr}\ddot{\theta}+\frac{d^2}{2}(C_f+C_r)\dot{\theta}+\frac{d^2}{2}(K_f+K_r)\theta=\frac{M_s v^2}{R} \text{ [17]} \tag{9}$$

where, I_{rr}, v, R, d are moment of inertia of body about roll centre, velocity of vehicle, radius of curvature and distance between roll centre and CoG position of body respectively.

$$\theta=\frac{M_s v^2}{R\left[I_{rr}s^2+\frac{d^2}{2}(C_f+C_r)s+\frac{d^2}{2}(K_f+K_r)\right]} \tag{10}$$

The step response of the Equation 10 is plotted in Fig 10. The graph shows that, at steady state the entire body will roll by 8 degree while having a turn. Which shows that the designed suspension performed adequately at the turn.

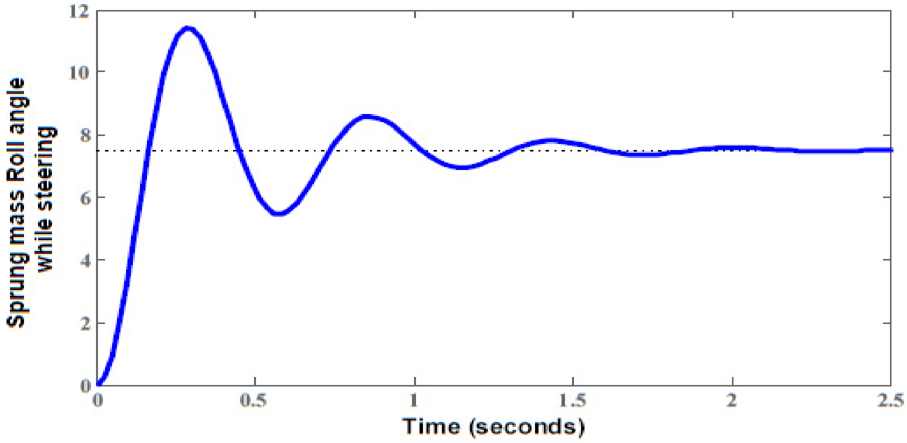

Figure 10. Time response of roll angle

7. Design of spring

From the static analysis, stiffness of spring (K) was calculated to be 40kN/m.

Pm=1/2(Pmax+Pmin), Pa=1/2(Pmax-Pmin) where Pmax and Pmin are the maximum and minimum forces acting on spring during wheel travel. Here 25.4mm of jounce and 25.4mm of re-bound was considered. The material generally used for spring damper is hardened steel.

$\tau_m = k_s\left(\frac{8P_m D}{\pi d^3}\right)$, $\tau_a = k\left(\frac{8P_a D}{\pi d^3}\right)$, C = D/d

ks = 1+ 0.5/C, $k = \frac{4C-1}{4C-4} + \frac{0.615}{C}$

Where ks, k are the design constants. C is spring index. D and d were inner and outer diameters of the spring respectively. By using machine design methodologies factor of safety of the spring is calculated.

G and S_{ut} are the modulus of rigidity and ultimate tensile strength of material respectively. Sse′= 0.22S_{ut}, S_{sy} = 0.45S_{ut} [21].

$$\frac{\tau_a}{\frac{S_{sy}}{f_s} - \tau_m} = \frac{S_{se}'}{2S_{sy} - S_{se}'} \tag{11}$$

Where fs is the factor of safety of the spring. Factor of safety of the spring should be 2<fs<3. Generally inner diameter of spring is taken to be 8mm. Hence fs is calculated in terms of C. For fs = 3, C comes out to be 6.5 and hence D = 52mm.

$$N = \frac{Gd^4}{8D^3 K_f} \tag{12}$$

Here N is number of coils in spring which comes out to be 8.

8. Results

Fig. 11 shows the plots of camber, toe and caster respectively obtained through kinematic analysis done in section 2 and 3.

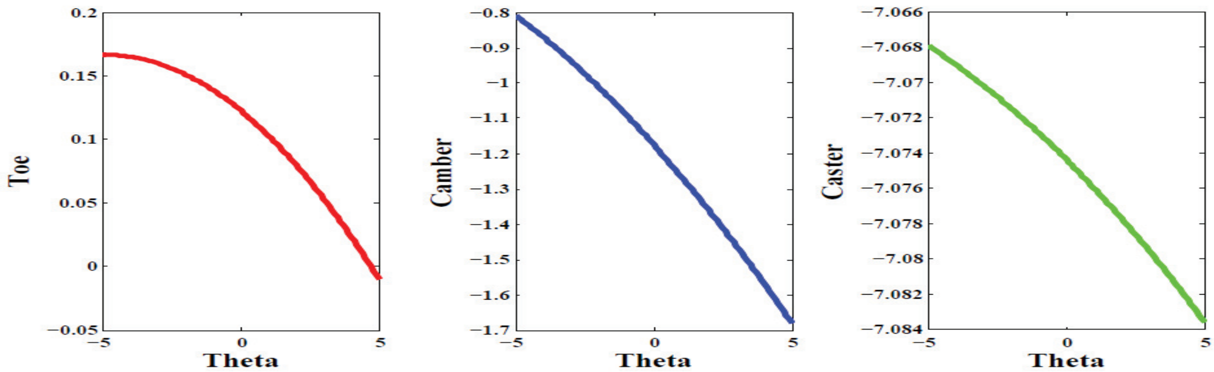

Figure 11. Variation in wheel alignment with wheel travel

Static analysis yields the required stiffness of spring along with sustainability of components from FE analysis. FE analysis was done by considering Al 6061 material for Bell Crank and Knuckle and Stainless Steel for A-Arms and Push Rod. Table 1 was the result of static analysis. Forces on each member is expressed as components along the axes. Those forces were applied on corresponding member.

	F_up_balljoint	F_low_balljoint	F_pushrod_BC	F_pushrod_L	Fspr
X	182.0982	-182.0982	372.8808	-369.1930	-420.0182
Y	4.5929	-396.9929	440.6647	-448.5127	5.6969
Z	191.9294	-191.9294	3.6878	-3.6878	6.7327

	F_up_balljoint	F_low_balljoint	F_pushrod_BC	F_pushrod_L	Fspr
X	958.1078	-1.9391e+03	2.6772e+03	-2.6507e+03	-3.0400e+03
Y	45.0682	-2.7919e+03	3.1881e+03	-3.1960e+03	41.2331
Z	1.6566e+03	-675.5668	26.4778	-26.4778	48.7300

Table 1. (a) Static analysis of suspension (b) Dynamic analysis suspension (mentioned in [14])

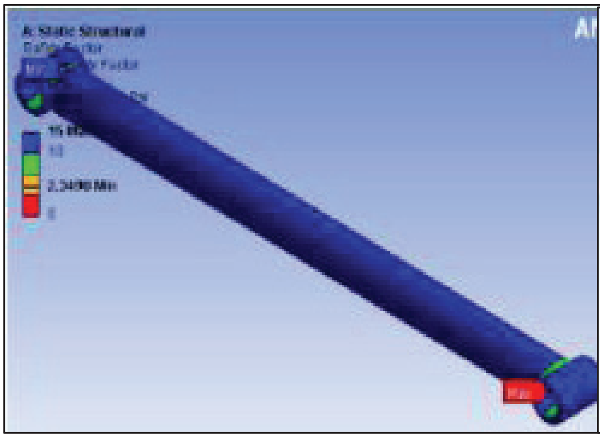

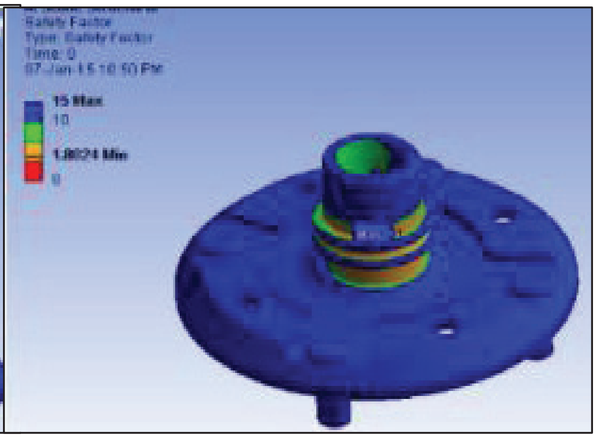

Push Rod (FoS: 2.3)

Hub (FoS: 1.8)

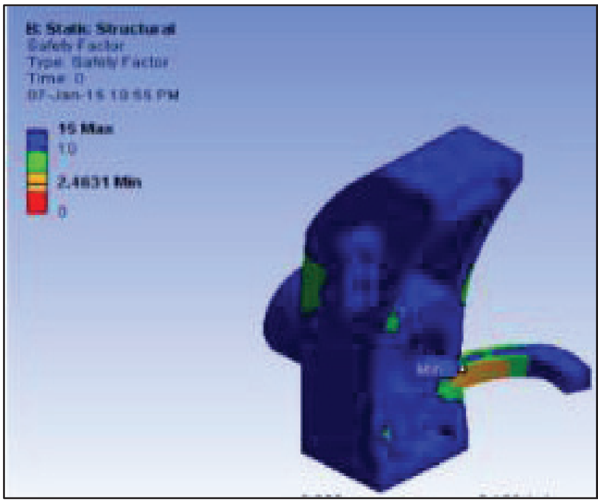

Knuckle (FoS: 2.4)

Lower A-Arm (FoS: 2.4)

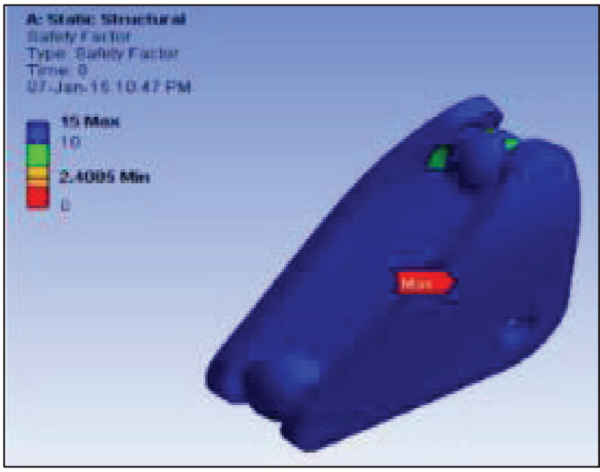

Bell Crank (FoS: 2.4)

Upper A-Arm (FoS: 2.4)

Figure 12. FEA using ANSYS Workbench®

Spring stiffness for the suspension was calculated to be 40000N/m with a damping ratio 0.7.

In entire analysis, our goal was to provide detail structure of the design of suspension. From kinematic analysis we found the kinematic parameters such as caster, camber, toe angles etc. Dynamic analysis of the kinematic linkages gave us stiffness of the spring for a particular ground clearance (static condition). Robustness, sustainability of the components were insured from their corresponding FE analysis. Vibration or ride analysis of the design showed us the effect of damping ratio on comfort and wheel deflection and in turn gave us the optimum value of coefficient of damping. After knowing the spring damper parameters we tested our design to check body roll for a particular speed and radius of curvature. Finally using design of spring data we found the required parameters for spring design.

APPENDIX A. Symbols Used

W = Weight of the vehicle

W_t = Weight of wheel assembly

W_{ua} = Weight of upper A arm

W_{la} = Weight of lower A arm

W_p = Weight of pushrod

M_u = Un-sprung mass

L_p = Length of pushrod

F_{ui} = Forces in i^{th} direction on upper A arm

F_{pb} = Force on push rod from bell crank

F_{li} = Forces in i^{th} direction on lower A-Arm

Z_s = Sprung mass displacement

Z_u = Un-sprung mass displacement

Z_r = Road profile

K_s = Stiffness of spring

C_s = Damping coefficient of damper

K_f, K_r = Stiffness of spring of front and rear suspension.

C_f, Cr = Coefficient of damping of front and rear suspension.

q = Damping ratio.

References

[1] SILVERSTONE 9-13 JULY 2014, formula student, Institute of Mechanical Engineers.
[2] http://www.sportskeeda.com/f1/pullrod-vs-pushrod-suspension-which-is-preferred.
[3] http://www.racecar-engineering.com/cars/university-of-southern-denmark/, SDU Vikings, University of Southern Denmark.
[4] https://sites.google.com/site/michigantechracing/video-gallery/the-car, 2013, Michigan Racing Formula SAE, F-151.
[5] http://www.racecar-engineering.com/cars/limerick-3/, April 2014, University of Limerick Racing, University of Limerick.
[6] Bos P.C.M., “Design of a Formula Student Race Car Spring-Damper System”, 0576519 CST2010.024.
[7] Gaffney III E. F., Salinas A. R., “Introduction to Formula SAE Suspension and spring design”, University of Missouri–Rolla, 971584.
[8] Salzano A., Klang E., “Design Analysis and fabrication of Formula SAE chassis”, 2009, Wolfpack motorsports, College of Engineering North Carolina state university.
[9] http://www.ndsu.edu/me/sae/formula/2013/formula.html, North Dakota State University BISON motorsports.
[10] http://web2.uwindsor.ca/fsae/car.html, 2010, Lancer Motor sports, University of Windsor.
[11] “Redesign of an FSAE Race Car’s Steering and Suspension System”, October 2011, University of Southern Queensland.
[12] Nazar R. J., “Vehicle Dynamics Theory and Application”, Springer, Library of Congress Control Number: 2007942198
[13] January D. B., “Steering Geometry and Caster Measurement”, SAE technical paper series 850219.
[14] Fenton J. (1980), Vehicle Body Layout and Analysis, Mechanical Engineering Publications Ltd. London
[15] Rajmani R., “Vehicle Dynamics and Control”, Springer, SPIN 11012085.
[16] Gillespie T.D., “Fundamentals of Vehicle Dynamics”, Society of Automotive Engineers.
[17] http://nptel.ac.in/courses/107106080/
[18] Mehmood A., Khan A. A., and Khan A. A., “Vibration Analysis Of Damping Suspension Using Car Models”, Sep. 2014, International Journal of Innovation and Scientific Research, Vol. 9 No. 2, pp. 202-211.
[19] Julian H. S., “An Introduction to Modern Vehicle Design”, 2001. Reed educational and professional publishing Ltd.
[20] Atherden M. J., Daniel W. J. T., “Formula SAE Shock Absorber Design”, 2004, The University of Queensland.
[21] Bhandari. V. B., “Design of Machine Elements”, 2010, TATA Mcgraw Hills.